Available online at www.sciencedirect.com
ScienceDirect
Journal of Photochemistry and Photobiology A: Chemistry 184 (2006) 78–85
Journal of Photochemistry and Photobiology A:Chemistry
www.elsevier.com/locate/jphotochem

Preparation of silica-modified TiO_2 and application to dye-sensitized solar cells

Toyohisa Hoshikawa, Tsugio Ikebe, Masashi Yamada, Ryuji Kikuchi, Koichi Eguchi *

Department of Energy and Hydrocarbon Chemistry, Graduate School of Engineering, Kyoto University, Nishikyo-ku, Kyoto 615-8510, Japan

Received 10 October 2005; received in revised form 19 January 2006; accepted 1 April 2006
Available online 18 April 2006

Abstract

Silica-modified titania (Si–TiO_2) was synthesized by the glycothermal method and applied for dye-sensitized solar cells (DSCs). Si–TiO_2 crystallized in anatase structure and was found to be thermally stable. Crystallite size of Si–TiO_2 became smaller as Si loadings in Si–TiO_2 increased, and Si–TiO_2 of small crystallite size adsorbed large amount of dyes on the surface. The photoelectrochemical conversion efficiency of the DSC using Si–TiO_2 was influenced mainly by the electron transfer between Si–TiO_2 particles. The Si–TiO_2-based DSCs showed a maximum in the conversion efficiencies when the crystallite size of Si–TiO_2 was around 15 nm, irrespective of the Si loadings. To improve the connectivity between Si–TiO_2 particles, Si–TiO_2 particles were mixed with TiO_2 sol, which was synthesized by the hydrothermal method. Dye-sensitized solar cells prepared using these pastes were able to reduce the influence of the resistance between the particles and improved their conversion efficiencies stemming from the increase of short circuit currents, since Si–TiO_2 could adsorb large amount of dyes.

Keywords: Dye-sensitized solar cell; Silica-modified titania; *I–V* curve; Impedance spectroscopy

1. Introduction

Recently, nanocrystalline semiconductor oxide-based dye-sensitized solar cells (DSCs) have been recognized as reasonable solar energy conversion devices [1]. DSCs consists of a nanocrystalline semiconductor film adsorbing dyes such as a Ru-bipyridyl complex, a redox couple such as I^-/I_3^-, and a counter electrode. The high efficiency of the DSC is achieved when a high surface area of the semiconductor film, which is necessary to adsorb large amount of dyes on its surface, is realized. Therefore, synthesis of semiconductor oxide having large surface area is one of the effective methods for preparation of the high performance DSC. At the present time, TiO_2 has been mainly used for high performance DSCs [2,3]. Although some kinds of nanocrystalline semiconductor oxide such as SnO_2 [4,5], ZnO [6–8], and Nb_2O_5 [9] were synthesized and applied to DSCs, their conversion efficiencies have not surpassed the original TiO_2-based DSC. Studies of DSCs using mixed-oxide electrodes have been mainly carried out on core-shell (bilayer) structure. This technique contributed to increase open circuit voltage (V_{oc}) in the case of TiO_2 core [10,11]. In the SnO_2-based electrodes, increase in both V_{oc} and short circuit current density (j_{sc}) have been reported and high conversion efficiency was recorded by SnO_2–ZnO system [11–13]. This improvement was explained as follows: the shell-oxide, which has more negative conduction band energy, covered the core-oxide and suppressed the recombination between the injected electrons in the core-oxide and electrolyte. In addition, the DSCs with composite oxides have also been investigated. Yoshikawa and co-workers prepared nanostructured TiO_2-based composite oxide such as TiO_2-ZrO_2 [14] and TiO_2-GeO_2 [15] with a surfactant assisted sol–gel method. They reported V_{oc} and j_{sc} improved in TiO_2-ZrO_2, and j_{sc} improved in TiO_2-GeO_2. This result indicates addition of small amount of another element to TiO_2 has possibility for improvement of DSCs.

This time, we focused on composite oxide, silica-modified titania (Si–TiO_2). This material has been reported by Iwamoto et al. as a high performance photocatalyst [16,17]. They reported that the Si–TiO_2 was directly synthesized by the reaction of raw materials, and the product possessed large surface area with

* Corresponding author. Tel.: +81 75 383 2519; fax: +81 75 383 2520.
E-mail address: eguchi@scl.kyoto-u.ac.jp (K. Eguchi).

1010-6030/$ – see front matter © 2006 Elsevier B.V. All rights reserved.
doi:10.1016/j.jphotochem.2006.04.001

small crystallite size and high thermal stability [17]. These features can lead to DSCs' advantages such as improvement of j_{sc} caused by adsorption of large amount of dyes on Si–TiO_2 particles. Therefore, we applied Si–TiO_2 to electrodes of DSCs in various conditions, and investigated that the effects of Si loading by impedance spectroscopy and potential of improvement in the performance of DSCs.

2. Experimental

2.1. Synthesis of TiO_2 and silica-modified TiO_2 powders

TiO_2 and silica-modified TiO_2 powders were synthesized by glycothermal method [18]. A 25 mL of titanium tetraisopropoxide (TTIP) and suitable amount of tetraethylorthosilicate (TEOS) were added into a glass tube with 100 mL of 1,4-butanediol, and this glass tube was set in the autoclave. A gap between the glass tube and the autoclave was filled with 1,4-butanediol. The sample was autoclaved for 2 h at 300 °C. After that, a valve on the autoclave was unclenched keeping its temperature at 300 °C to remove the solvent. The resultant powders were calcined at or above 400 °C for 2 h to remove the organic solvent on surface of powders completely. Hereafter, the powder prepared by TTIP and TEOS containing *x* at.% of Si, is abbreviated as *x* at.% Si–TiO_2.

2.2. Preparation of TiO_2 and Si–TiO_2 pastes

Two kinds of TiO_2 and Si–TiO_2 pastes for electrodes of DSCs were prepared. One was consisting of TiO_2 or Si–TiO_2 powders alone. One gram of TiO_2 or Si–TiO_2 powder, 30 wt.% polyethyleneglycol 20000 (PEG20000), and 5 mL of 0.1 M HNO_3 aqueous solution were added and ground vigorously in an automatic mortar, until the paste became reasonably viscous. After that, pastes were dispersed for 30 min by ultrasonication.

The other was that TiO_2 sol synthesized by the hydrothermal method was mixed with these powders. TiO_2 sol was prepared based on the method reported before [19]. A 125 mL of TTIP was dropped into 750 mL of a 0.1 M HNO_3 aqueous solution under stirring vigorously at room temperature. After that, the slurry was heated at 80 °C and stirred vigorously for 8 h. The resultant solution was then filtered, and distilled water was added into the filtrate to adjust the total volume to 700 mL. After that, the solution was autoclaved under hydrothermal condition for 12 h at 230 °C. The growth of particles in the solution occurred during the autoclaving, and the particles were redispersed with ultrasonic wave. The colloidal suspension was concentrated with a rotary evaporator to a final TiO_2 concentration of 11 wt.%. A 30 wt.% of TiO_2 or Si–TiO_2 and PEG20000 were added in this colloidal sol (10 mL) and ground vigorously in an automatic mortar.

2.3. Characterization of TiO_2 and Si–TiO_2 powders and electrodes

Crystallite phases of TiO_2 and Si–TiO_2 powders were identified by X-ray diffraction (RINT1400, Rigaku Co., Ltd.) and crystallite sizes were calculated from their patterns by Scherrer's equation. Presence of Si in Si–TiO_2 powders was confirmed by FT-IR (FT/IR-410, JASCO Co., Ltd.), and XPS (ESCA-850, Shimadzu Co., Ltd.). The charging effect in XPS was corrected by adjusting the binding energy of the main C 1s peak to 284.6 eV. Amount of dyes on electrodes were measured by inductively coupled plasma spectroscopy (ICP). Dyes on electrodes were dissolved with 10 mL of 0.1 M NaOH aqueous solution. The amount of TiO_2 and Si–TiO_2 on electrodes was also estimated from Ti concentration obtainedetermined by ICP.

2.4. Assembly of dye-sensitized solar cells

Two parallel edges of F-doped SnO_2 glass (FTO) were covered with adhesive tape (thickness: 50 μm) to control the thickness of the TiO_2 or Si–TiO_2 film. The paste was applied to one of the free edges of the FTO and spread by sliding a glass rod on the tape-covered edges. The thin film of TiO_2 or Si–TiO_2, thus obtained after calcination, was ca. A 20 μm thick. After the electrode was dried in air, it was calcined for 1 h at 500 °C in air. A dye, *cis*-bis(isothiocyanato)bis(2,2′-bipyridyl-4,4′-dicarboxylato)-ruthenium(II) bis-tetrabutylammonium, generally called N719, was used as a sensitizer. Dye adsorption on the TiO_2 and Si–TiO_2 electrodes were carried out by immersing the electrode into an ethanol solution with a dye concentration of 3×10^{-4} M (M = mol dm^{-3}). Electrode area was about 0.25 cm^2. As a counter electrode, a thin Pt layer was deposited on In-doped SnO_2 glass substrate (ITO) by sputter technique. A 50 μm thick thermoplastic resin film (Mitsui-Du Pont Polychemical Co., Ltd.) with a 7 mm × 7 mm window was sandwiched between these two electrodes, and then the assembly was heated on a hot plate to tighten the seal. The electrolyte solution was filled between the two electrodes. As the electrolyte solution 0.6 M 1-propyl 2,3-dymethylimidazolium iodide (DMPImI), 0.1 M LiI, 0.5 M 4-*t*-butylpyridine (*t*-BuPy) and 0.05 M I_2 in methoxyacetonitrile (MeAN) were employed.

Hereinafter, the DSC based on TiO_2 is abbreviated as Ti-DSC, Ti-DSC based on TiO_2 calcined at 500 °C as Ti-500, the DSC based on Si–TiO_2 as Si-DSC, and Si-DSC based on 5 at.% Si added Si–TiO_2 calcined at 600 °C as 5-Si-600.

2.5. Photoelectrochemical measurements

Current–voltage characteristics measurement (*I–V* measurement) and ac impedance spectroscopy were carried out as photoelectrochemical measurements. A potentiostat (Solartron 1287) and frequency response analyzer (Solartron1260) were used for these measurements. The light source was a solar simulator (K-0206, Bunko Keiki), and the light power was calibrated by silicon photodiode (BS-520, Bunko Keiki). In this experiment, *I–V* and impedance measurements were carried out without the mask for cutting off ambient light. The impedance measurement of cells was recorded over a frequency range of 0.01–100,000 Hz with ac amplitude of 10 mV. The measurement was carried out after open circuit voltage became stable (about 15 min).

3. Results and discussion

3.1. Characterization of TiO_2 and Si–TiO_2 powders

The XRD patterns of silica-modified TiO_2, with Si loadings of 0–5 at.%, are shown in Fig. 1. All samples had the anatase structure and other peaks were not obtained, as reported previously [16]. Presence of Si in Si–TiO_2 powders could be confirmed by IR and XPS. Fig. 2 shows IR spectra of Si–TiO_2 with different Si loadings. The spectra in Fig. 2 consist of two main absorption bands, which are attributed to characteristic bonds of Si–O–Si asymmetric stretching (near 1070 cm^{-1}) and Ti–O–Si asymmetric stretching (near 950 cm^{-1}), in Si–TiO_2 [20,21]. These absorption bands became conspicuous, as Si loadings in Si–TiO_2 increase. Fig. 3 shows Si 2p spectra of Si–TiO_2 with different Si loadings. In Si 2p spectra, main peak was observed at 101.5 eV, and this peak was larger with an increase in the amount of Si loaded. This binding energy is smaller than that of pure SiO_2 (103.6 eV). Iwamoto et al. have explained that a low binding energy of Si 2p was due to the decrease of the effective positive charge on the Si atoms. Since electronegativity of Si is higher than that of Ti, the formation of the Si–O–Ti bonds causes a less effective positive charge on the Si atoms, as compared to that of pure SiO_2. This result suggests that the strong interaction of Si atoms with TiO_2 lattice [17].

The crystallite sizes of Si–TiO_2 with various amount of Si calcined at various temperatures for 2 h are shown in Fig. 4. The crystallite size was calculated by Scherrer's equation. As Si loadings increased, the crystallite size of Si–TiO_2 became small. The crystallite size was small for the sample containing larger amount of Si, even after the calcination at high temperatures. Iwamoto et al. reported that increase in Si loadings retarded the grain growth of anatase and trans formation of anatase to rutile, and that addition of Si decreased the OH group concentration on the surface of the Si–TiO_2, which contributed to improvement of the thermal stability of Si–TiO_2 due to decrease in the surface energy of Si–TiO_2 particles [16,17]. This result indicates that the addition of Si to TiO_2 can create the smaller particle size of Si–TiO_2 at the same calcination temperature. These particles are expected to adsorb larger amount of dye-adsorption on particles as semiconductor electrodes of DSCs.

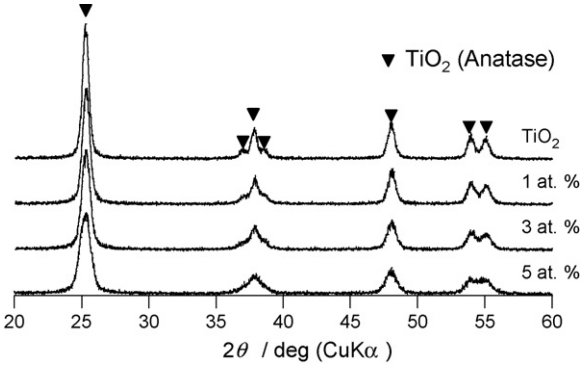

Fig. 1. XRD patterns of TiO_2 and silica-modified TiO_2 calcined at 600 °C for 2 h; 1, 3, and 5 at.% Si were added in Si–TiO_2.

Fig. 2. IR spectra of TiO_2 and silica-modified TiO_2 calcined at 600 °C for 2 h; 1, 3, and 5 at.% Si were added in Si–TiO_2.

3.2. Dye-adsorption on silica-modified TiO_2 electrodes

The relation between amount of dyes on Si–TiO_2 electrodes and their crystallite sizes is shown in Fig. 5. Amount of dyes on the electrodes were expressed as number of moles per unit weight of TiO_2 and Si–TiO_2 electrodes. Higher Si loadings of Si–TiO_2 electrodes, whose powders had smaller crystallite sizes compared with TiO_2, enabled to adsorb more amount of dyes on electrodes. In addition, inverse of crystallite sizes of TiO_2 and Si–TiO_2 and amount of dyes on their electrodes have linear relation. This result suggests that dyes adsorb uniformly on the outer surface of original TiO_2 and Si–TiO_2 particles. And Fig. 5

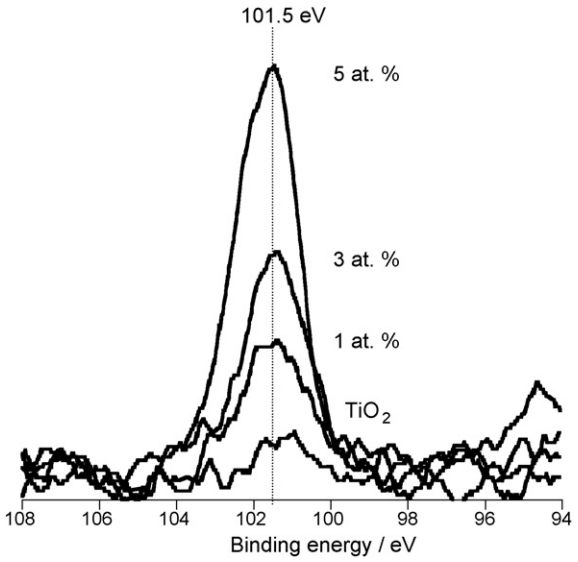

Fig. 3. Si 2p spectra of TiO_2 and silica-modified TiO_2 calcined at 600 °C for 2 h; 1, 3, and 5 at.% Si were added in Si–TiO_2.

showed plots of TiO_2 and Si–TiO_2 were on the same sequence. This indicates ability for adsorption of dyes on Si–TiO_2 was equal to that on TiO_2. Larger amount of dyes on Si–TiO_2 can lead to accomplish higher short circuit current in DSCs.

3.3. Si–TiO_2-based dye-sensitized solar cells

Fig. 6 shows (a) *I–V* curves and (b) impedance spectra of TiO_2 (Ti-500) and 5 at.% Si–TiO_2 (5-Si-500)-based dye-sensitized solar cells. Open circuit voltage, j_{sc}, fill factor and conversion efficiency were 0.669 V, 10.6 mA cm^{-2}, 0.703, and 4.99% in Ti-500 and 0.629 V, 3.69 mA cm^{-2}, 0.726, and 1.69% in 5-Si-500, respectively. The impedance spectrum of the Ti-500 consisted of four components. The ohmic resistance, which was represented

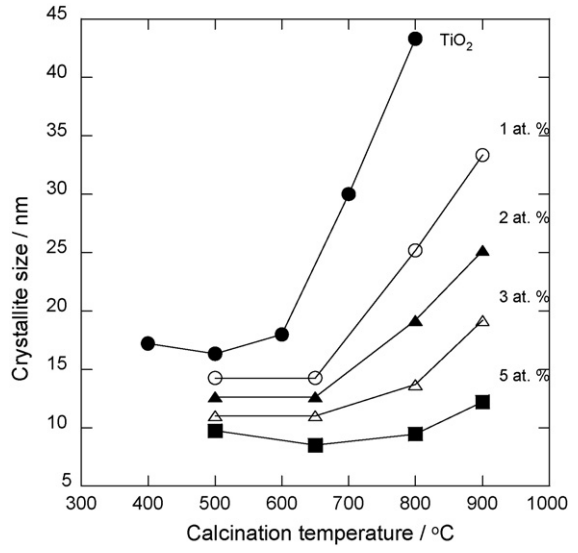

Fig. 4. The relation between crystallite size of TiO_2 and silica-modified TiO_2 calcined various temperatures for 2 h; 1, 2, 3, and 5 at.% Si were added in Si–TiO_2.

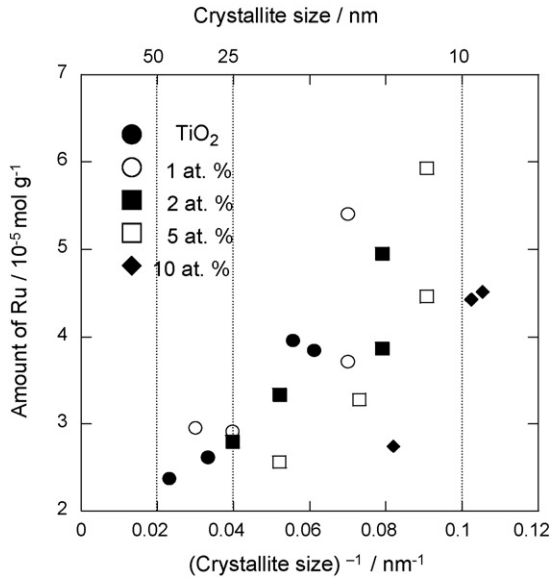

Fig. 5. The relation between amount of dyes on TiO_2 and Si–TiO_2 electrodes and their crystallite sizes; 1, 2, 5, and 10 at.% Si were added in Si–TiO_2. Powders were calcined at various temperatures to adjust the crystallite sizes.

0 to Z'-intercept of impedance spectra at high frequency side (left side), did not appear as semicircle due to its very short time constant. This resistance includes the sheet resistance at glass substrate and solvent resistance in electrolyte. The arcs at 7000, 10, and 0.5 Hz have been attributed to electron transfer at Pt| electrolyte interface, at dye adsorbing TiO_2| electrolyte interface, and diffusion of I_3^- in electrolyte, respectively [22–24].

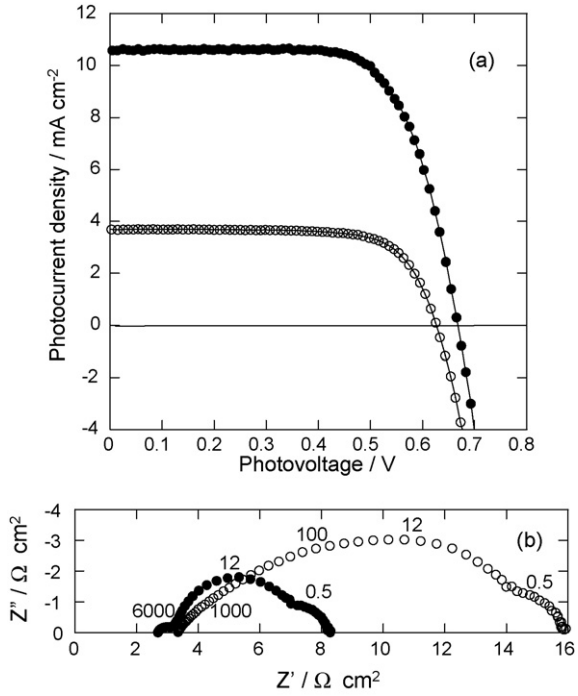

Fig. 6. (a) *I–V* curves and (b) impedance spectra at V_{oc} of TiO_2 and 5 at.% Si–TiO_2-based dye-sensitized solar cells under 100 mW cm^{-2} light irradiation. Si–TiO_2 powders were calcined at 500 °C. Numbers in impedance spectra stand for frequency at each point. (●) TiO_2; (◯) 5 at.% Si–TiO_2.

In the impedance spectrum of 5-Si-500, the impedance component around 1000–100 and at 10 Hz were larger than those in the spectrum of Ti-500. The large component around 1000–100 Hz, which is often observed when calcination temperature of the TiO_2 electrode is lower than 400 °C [25], indicates that the electron transfer in Si–TiO_2 electrode was not smooth due to weak connectivity between the particles. Another large arc at 10 Hz, which becomes small when the amount of dyes on TiO_2 and light intensity increase [24,25], indicates that electron density in the Si–TiO_2 electrode was low. These impedance components represent low short circuit current and low conversion efficiencies in the Si-DSCs.

Fig. 7 shows (a) *I–V* curves and (b) impedance spectra of dye-sensitized solar cells based on 5 at.% Si–TiO_2 calcined at 500, 650, 800, and 900 °C. Open circuit voltage increased slightly with higher calcination temperature (0.629, 0.628, 0.633, and 0.653 V), and fill factor was almost the same (0.726, 0.727, 0.721, and 0.729). Short circuit current density had the maximum at 800 °C (9.05 mA cm^{-2}). Consequently, the sample 5-Si-800 showed the best conversion efficiency in these DSCs. The impedance spectrum of 5-Si-800 was smaller than that of other three DSCs. The impedance spectra of DSCs consisting of

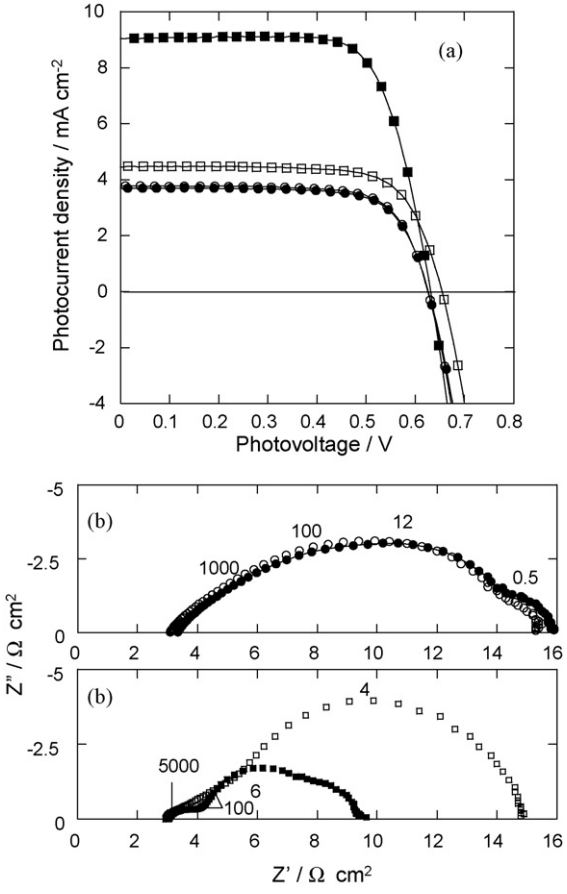

Fig. 7. (a) *I–V* curves and (b) impedance spectra at V_{oc} of TiO_2 and 5 at.% Si–TiO_2-based dye-sensitized solar cells under 100 mW cm^{-2} light irradiation. Si–TiO_2 powders were calcined at 500, 650, 800, and 900 °C. Numbers in impedance spectra stand for frequency at each point. (●) 500 °C; (◯) 600 °C; (■) 800 °C; (□)900 °C.

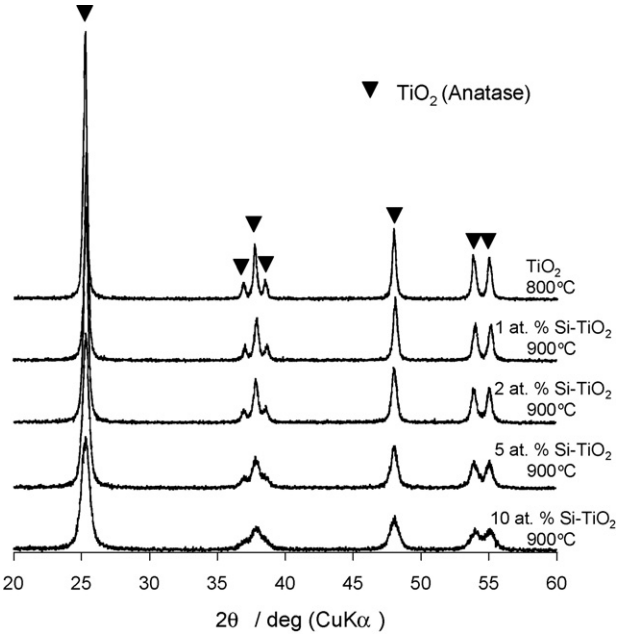

Fig. 8. XRD patterns of TiO_2 calcined at 800 °C and silica-modified TiO_2 calcined at 900 °C for 2 h; 1, 2, 5 and 10 at.% Si were added in Si–TiO_2.

5-Si-500 and 5-Si-600 have almost the same spectra. Therefore, the low efficiencies and low j_{sc} obtained from these DSCs can be ascribed to the low connectivity between particles and low electron density in Si–TiO_2 as mentioned above. The sample 5-Si-900 has a relatively small arc at 100 Hz and large one arc at 10 Hz. Fig. 8 shows XRD patterns of TiO_2 and Si–TiO_2 calcined at high temperature. Even the TiO_2 calcined at 800 °C and Si–TiO_2 calcined at 900 °C consisted of only anatase phase, hence it is not necessary to consider the effects of crystallite phase on *I–V* characteristics of DSCs in this experiment. Impedance spectrum of 5-Si-900 indicates that the electric connectivity between the particles is sufficient to transfer injected electrons. The number of the injected electrons, however, becomes less due to decrease of dyes on the high-temperature calcined Si–TiO_2 and leads to low j_{sc}. This result suggests that Si–TiO_2 powders have an optimal calcination temperature for good performance DSCs.

I–V characteristics of various kinds of Si-DSCs calcined at different temperatures are shown in Fig. 9. Open circuit voltage of the Ti-DSC increased with calcination temperature was higher. The V_{oc} of Si-DSCs slightly increased as calcination temperature was raised. And the V_{oc} decreased as Si loadings increased. Small particle size and/or large Si loadings can contribute to decrease of V_{oc}. Short circuit current and conversion efficiency of these DSCs have almost the same tendency to calcination temperatures. This indicates that conversion efficiencies of these Si-DSCs are mainly controlled by short circuit current. Maximum values of short circuit current and conversion efficiencies shifted to higher calcination temperatures as Si loadings were increased. Fill factor did not exhibit tendency to Si loadings and calcination temperatures.

Fig. 10 shows relation between crystallite size of TiO_2 and Si–TiO_2 for DSCs and their *I–V* characteristics. A trend can be found for open circuit voltages to increase with an increase in

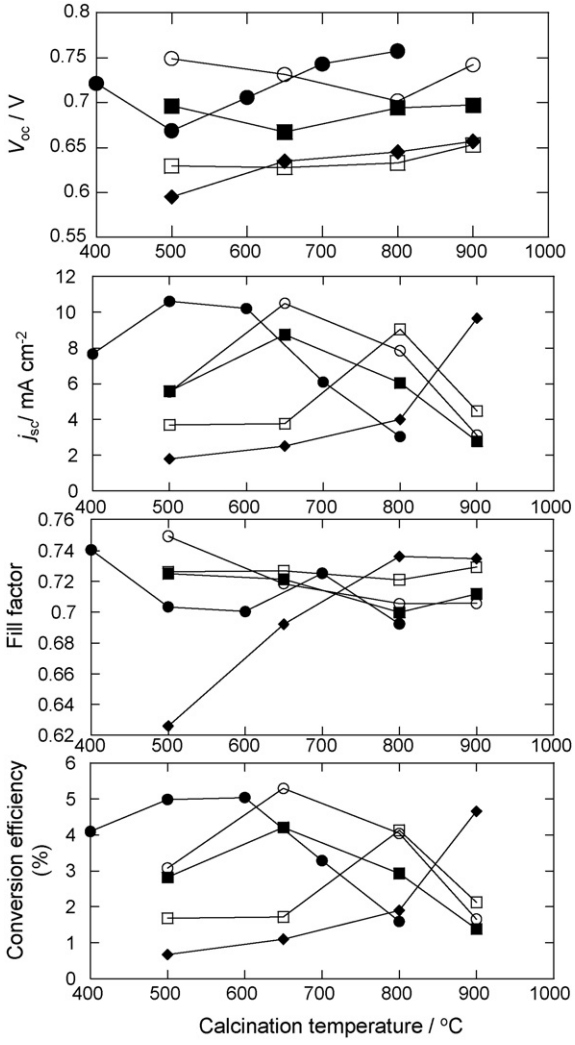

Fig. 9. Relations between calcination temperatures and *I–V* characteristics of TiO_2 and 1, 2, 5, and 10 at.% Si–TiO_2-based DSCs under 100 mW cm^{-2} light irradiation. (●) TiO_2; (◯) 1 at.% Si; (■) 2 at.% Si; (□) 5 at.% Si; (♦) 10 at.% Si.

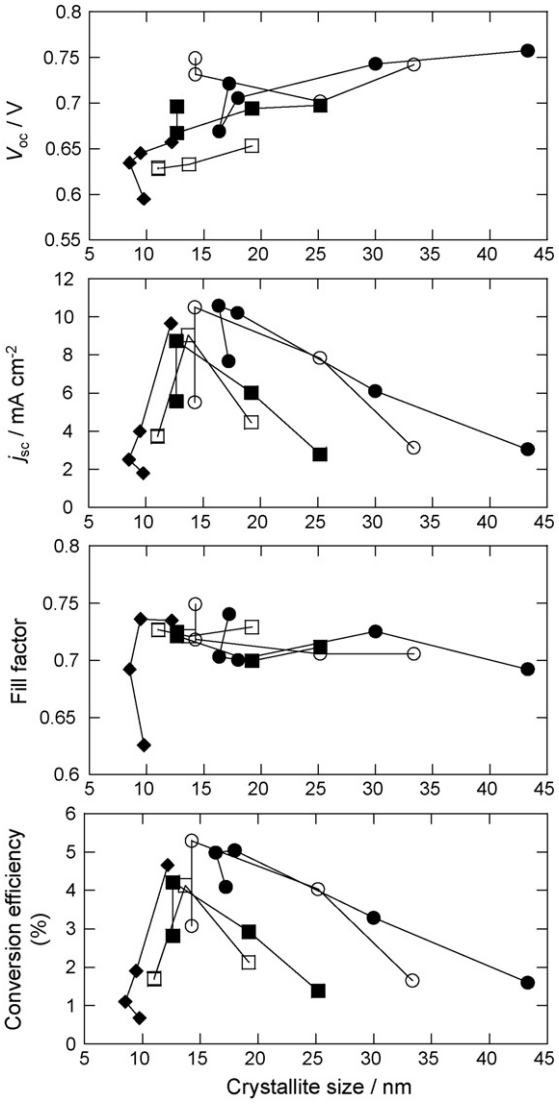

Fig. 10. Relations between crystallite sizes and *I–V* characteristics of TiO_2 and 1, 2, 5, and 10 at.% Si–TiO_2-based DSCs under 100 mW cm^{-2} light irradiation. (●) TiO_2; (◯) 1 at.% Si; (■) 2 at.% Si; (□) 5 at.% Si; (♦) 10 at.% Si.

crystallite sizes of TiO_2 and Si–TiO_2. It is considered that very small semiconductor oxide particles like nanoparticles are hard to keep the electric barrier (space charge layer) in their interface due to their small size. This electric barrier serves as inhibition of back reaction such as the reaction between the injected electrons in the electrode and oxidized electrolyte. As a consequence, electron densities in the electrode and Fermi level increase and lead to increase in the open circuit voltage. Large particles are easier to create the electric barrier than small ones, and therefore, DSCs with particles of large crystallite size have high open circuit voltage [25]. The highest short circuit current and conversion efficiencies were obtained around 15 nm of crystallite size. It is difficult for excessively small particles to sustain the electrode film, and there are often cracks on the film and peeling from FTO. The film consisting of large particles does not have large surface area, therefore, the amount of dyes on the electrode decreases with an increase of the crystallite size.

Fig. 11 is *I–V* curves and impedance spectra of the Ti-DSC and Si-DSCs that displayed best conversion efficiencies in the respective calcination temperatures in Fig. 9. The DSCs based on TiO_2, 1, 5, and 10 at.% Si–TiO_2 exhibited the maximum conversion efficiencies at calcinations temperature of 600, 650, 800, and 900 °C, respectively, in this preparation condition. The *I–V* characteristics of 1-Si-650 was the almost same as that of Ti-600. The V_{oc} and j_{sc} of 5-Si-800 and 10-Si-900 were inferior to those of Ti-600. In the impedance spectra of these DSCs, the impedance of Ti-DSC consisted of three arcs and that of Si-DSC consisted of four components, although total impedances were almost the same. A new impedance component appeared at around 500 Hz in Si-DSC, and this impedance became large as Si loadings were increased. This suggests electrons in the electrode of high Si contents do not transfer smoothly due to poor connectivity between the particles. Arcs around 10 Hz became somewhat small with increase of Si loadings. This phenomenon meant that more dyes were adsorbing on Si–TiO_2 than TiO_2 the more electrons were injected from dyes into the Si–TiO_2 electrode. These results indicate that if the contribution of the

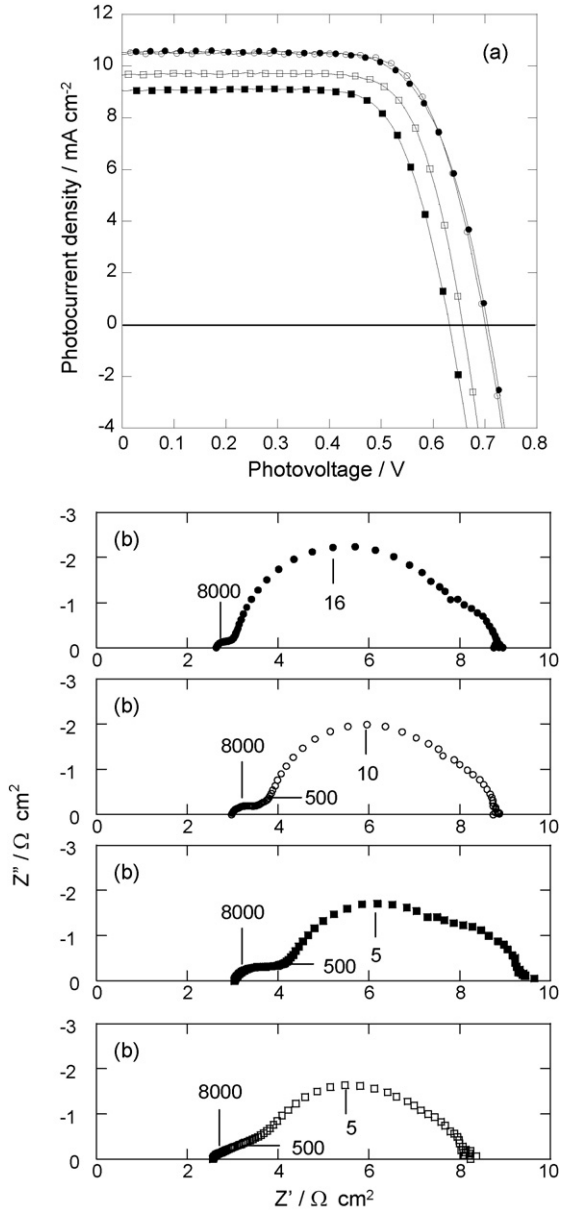

Fig. 11. (a) *I–V* curves played the best performances in TiO_2 and Si–TiO_2-based DSCs in Fig. 9 or Fig. 10 and (b) their impedance spectra. Numbers in impedance spectra stand for frequency at each point. (●) Ti-600; (◯) 1-Si-650; (■) 5-Si-800; (□) 10-Si-900.

impedance around 500 Hz on the Si-DSC is lowered, the conversion efficiency of these DSCs are expected to improve.

To improve the connectivity of Si–TiO_2 electrodes, TiO_2 sol were mixed with Si–TiO_2 powders. *I–V* curves in Fig. 12 showed that DSCs based on TiO_2 sol with TiO_2 and Si–TiO_2 powders have higher j_{sc} than that of the DSC without the additive. The DSCs with Si–TiO_2 additives recorded the j_{sc} equivalent to or higher than that with TiO_2 additives. Their impedance spectra in Fig. 12 had the relatively small arcs at high frequency range (left arcs), compared with the spectra in Fig. 11. This means that the electron transfer in electrodes becomes more smoothly by mixing with TiO_2 sol. Arcs at 10 Hz became small as their j_{sc} increased. Similar behavior was observed when light intensity

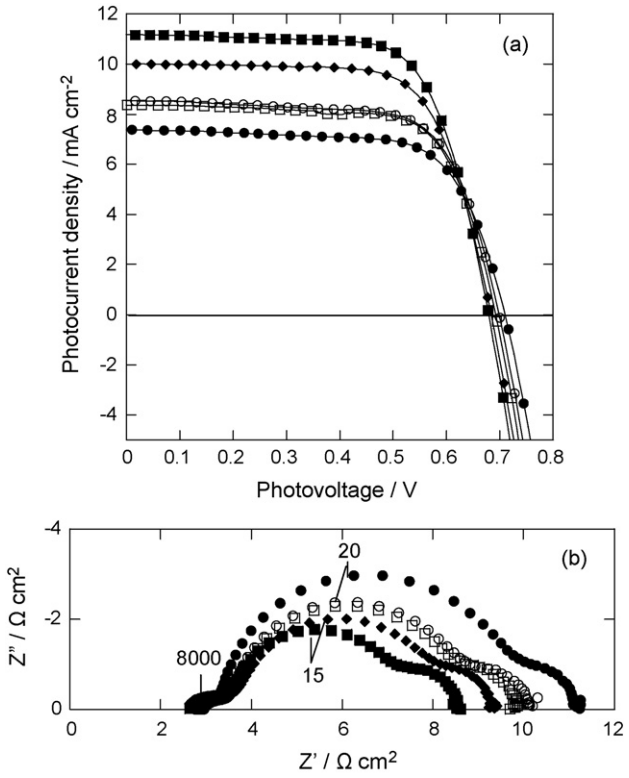

Fig. 12. (a) *I–V* curves and (b) impedance spectra at V_{oc} of TiO_2 sol-based DSCs under 100 mW cm^{-2} light irradiation. 30 wt.% of TiO_2 and 1, 3, and 5 at.% Si–TiO_2 calcined at 600 °C were added in TiO_2 sol. (●) without additive; (◯) TiO_2; (■) 1 at.% Si; (□) 3 at.% Si; (♦) 10 at.% Si.

was changed. The arc at 10 Hz became small as light intensity was raised [22]. Therefore, the behavior in the impedance spectra in Fig. 12 was caused by difference in number of the injected electrons in the electrode. Higher performances of DSCs containing Si–TiO_2 were realized, since Si–TiO_2 powders were able to adsorb more amount of dyes on the surface. j_{sc} and the reciprocal of the resistance characterized by the arc at around 10 Hz displayed some correlations, as shown in Fig. 13. This

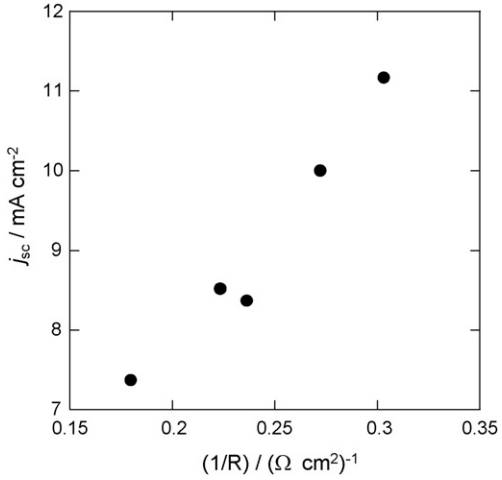

Fig. 13. The relation between impedance components around 10 Hz of DSCs and j_{sc} shown in Fig. 12.

result suggests that j_{sc} of these DSCs were mainly affected by the impedance at 10 Hz, and the impedances around 500 Hz, whose influence was observed in Fig. 11, did not affect so significantly their conversion efficiencies. TiO_2 sol containing Si–TiO_2 powders-based DSCs could improve the connectivity in electrodes and utilize the advantage of Si–TiO_2.

4. Conclusions

Si–TiO_2 with various Si loadings were synthesized by the glycothermal method and applied to dye-sensitized solar cells. These Si–TiO_2 powders had anatase structure and their crystallite size became small, as the Si loadings increased. This suggested that Si–TiO_2 had high thermal stability compared with TiO_2. Consequently, small particles were obtained from Si–TiO_2 and these particles adsorbed large amount of dye on their surface. Conversion efficiencies and j_{sc} of Si-DSCs were lower than those of Ti-DSCs and the maximum values were obtained when crystallite size of Si–TiO_2 was around 15 nm. Impedance spectra of these DSCs had arcs around 500 Hz and implied that conversion efficiencies of these DSCs were influenced by the electron transfer in the Si–TiO_2 electrodes. To improve the connectivity between Si–TiO_2 particles, Si–TiO_2 particles were mixed with TiO_2 sol, which was synthesized by the hydrothermal method. Dye-sensitized solar cells using these pastes were able to lower the resistance between particles and to improve their conversion efficiencies derived from the increase of short circuit currents. This improvement was due to large amount of dyes adsorbing on Si–TiO_2 surface.

Si-DSCs in this experiment showed that conversion efficiencies of DSCs were influenced strongly by the morphology of Si–TiO_2 electrode such as crystallite size rather than electrochemical properties of Si–TiO_2. Therefore, optimizations of preparation methods have possibility to improve conversion efficiencies of Si-DSCs.

Acknowledgment

This work was supported by a JSPS Fellowship (15005584, 2003) from the Japan Society for the Promotion of Science.

References

[1] B. O'Regan, M. Grätzel, Nature 353 (1991) 737–739.
[2] M.K. Nazeeruddin, A. Kay, I. Rodicio, R. Humphry-Baker, E. Müller, P. Liska, N. Vlachopoulos, M. Grätzel, J. Am. Chem. Soc. 115 (1993) 6382–6390.
[3] M. Grätzel, J. Photochem. Photobiol. C 4 (2003) 145–153.
[4] Y. Tachibana, K. Hara, S. Takano, K. Sayama, H. Arakawa, Chem. Phys. Lett. 364 (2002) 297–302.
[5] S. Chappel, A. Zaban, Sol. Energy Mater. Sol. C 71 (2002) 141–152.
[6] T. Yoshida, H. Minoura, Adv. Mater. 12 (2000) 1219–1222.
[7] K. Keis, E. Magnusson, H. Lindström, S.-E. Lindquist, A. Hagfeldt, Sol. Energy Mater. Sol. C 73 (2002) 51–58.
[8] M. Law, L.E. Greene, J.C. Johnson, R. Saykally, P. Yang, Nat. Mater. 4 (2005) 455–459.
[9] P. Guo, M.A. Aegerter, Thin Solid Films 351 (1999) 290–294.
[10] S.G. Chen, S. Chappel, Y. Diamant, A. Zaban, Chem. Mater. 13 (2001) 4629–4634.
[11] A. Kay, M. Grätzel, Chem. Mater. 14 (2002) 2930–2935.
[12] K. Tennakone, G.R.R. Kumara, I.R.M. Kottegoda, V.P.S. Perera, Chem. Commun. 1 (1999) 15.
[13] S. Ito, Y. Makari, T. Kitamura, Y. Wada, S. Yanagida, J. Mater. Chem. 14 (2004) 385–390.
[14] A. Kitiyanan, S. Ngamsinlapasathian, S. Pavasupree, S. Yoshikawa, J. Solid State Chem. 178 (2005) 1044–1048.
[15] A. Kitiyanan, T. Kato, Y. Suzuki, and S. Yoshikawa, J. Photochem. Photobiol. A 179 (2006) 130–134.
[16] S. Iwamoto, W. Tanakulrungsank, M. Inoue, K. Kagawa, P. Praserthdam, J. Mater. Sci. Lett. 19 (2000) 1439–1443.
[17] S. Iwamoto, S. Iwamoto, M. Inoue, H. Yoshida, T. Tanaka, K. Kagawa, Chem. Mater. 17 (2005) 650–655.
[18] S. Iwamoto, K. Saito, M. Inoue, Nano Lett. 1 (2001) 417–421.
[19] V. Shklover, M.-K. Nazeeruddin, S.M. Zakeeruddin, C. Barbé, A. Kay, T. Haibach, W. Steurer, R. Hermann, H.-U. Nissen, M. Grätzel, Chem. Mater. 9 (1997) 430–439.
[20] H. Chun, W. Yizhong, T. Hongxiao, Appl. Catal. 30 (2001) 277–285.
[21] Y. Zhao, L. Xu, Y. Wang, C. Gao, D. Liu, Catal. Today 93–95 (2004) 583–588.
[22] T. Hoshikawa, R. Kikuchi, K. Sasaki, K. Eguchi, Electrochemistry 70 (2002) 675–680.
[23] R. Kern, R. Sastrawan, J. Ferber, R. Stangl, J. Luther, Electrochim. Acta 47 (2002) 4213–4225.
[24] T. Hoshikawa, M. Yamada, R. Kikuchi, K. Eguchi, J. Electrochem. Soc. 152 (2005) E68–E73.
[25] A. Hagfeldt, M. Grätzel, Chem. Rev. 95 (1995) 49–68.